

# On the role of shear in cosmological averaging

---

**Maria Mattsson**<sup>1,2,\*</sup>, **Teppo Mattsson**<sup>2,†</sup>

<sup>1</sup> *Physics Department and Helsinki Institute of Physics, P.O.Box 64, FIN-00014  
University of Helsinki, Finland*

<sup>2</sup> *Department of Physics and Astronomy, University of Canterbury, Private Bag 4800,  
Christchurch 8140, New Zealand*

ABSTRACT: Using the spherically symmetric inhomogeneous Lemaitre-Tolman-Bondi dust solution, we study how the shear and the backreaction depend on the sharpness of the spatial transition between voids and walls and on the size of the voids. The voids considered here are regions with matter density  $\Omega_0 \simeq 0$  and expansion rate  $H_0 t_0 \simeq 1$ , while the walls are regions with matter density  $\Omega_0 \simeq 1$  and expansion rate  $H_0 t_0 \simeq 2/3$ . The results indicate that both the volume-average shear and the variance of the expansion rate grow proportional to the sharpness of the transition and diverge in the limit of a step function, but, for realistic-sized voids, are virtually independent of the size of the void. However, the backreaction, given by the difference of the variance and the shear, has a finite value in the step-function limit. By comparing the exact result for the backreaction to the case where the shear is neglected by treating the voids and walls as separate Friedmann-Robertson-Walker models, we find that the shear suppresses the backreaction by a factor of  $(r_0/t_0)^2$ , the squared ratio of the void size to the horizon size. This exemplifies the importance of using the exact solution for the interface between the regions of different expansion rates and densities. The suppression is justified to hold also for a network of compensated voids, but may not hold if the universe is dominated by uncompensated voids.

KEYWORDS: Inhomogeneous Cosmological Models, Averaging in General Relativity, Cosmology, Gravitation.

---

\*E-mail: maria.ronkainen@helsinki.fi

†E-mail: teppo.mattsson@canterbury.ac.nz

---

## Contents

<b>1. Introduction</b>	<b>1</b>
<b>2. LTB solution</b>	<b>2</b>
2.1 The void-wall model	4
2.2 Small $k(r)$ expansion	4
<b>3. Scalar averaging</b>	<b>5</b>
3.1 Averaging in the LTB model	6
<b>4. Shear</b>	<b>6</b>
<b>5. Backreaction</b>	<b>8</b>
5.1 Backreaction in 0th order of $k(r)$	8
5.2 Backreaction in 1st order of $k(r)$	9
5.3 Comparison with a model that consists of two disjoint FRW solutions	10
5.4 Uncompensated voids	11
<b>6. Conclusions</b>	<b>13</b>

---

## 1. Introduction

An unresolved issue in cosmology is the effect of the structure formation on the cosmological observations beyond perturbative analysis of the Friedmann-Robertson-Walker or FRW models [1–4]. On account of the increased precision of these observations and the cosmic acceleration that they seem to indicate [5–7], the evaluation of this effect has become important [8–11]. A way to estimate the effect of the cosmic structures is via a backreaction term that arises by averaging inhomogeneous scalar quantities on spatial hypersurfaces [12]. The backreaction thus obtained is given by the variance of the expansion rate minus the non-negative average shear.

A simplification in some estimates of the cosmological backreaction is based on partially or fully neglecting the shear on the interface between regions of different expansion rates [13–15]: these studies have found a significant amount of backreaction. On the other hand, perturbative studies that do not neglect the shear have suggested the backreaction to be insignificant [16–19]; however, see Ref. [4] for a recent discussion on the possible shortcomings of the perturbative approach in the backreaction problem. In this paper, we consider the issue within exact general relativity by studying:

1. How the sharpness of the spatial transition between the voids (where  $\Omega_0 \simeq 0$  and  $H_0 t_0 \simeq 1$ ) and the walls (where  $\Omega_0 \simeq 1$  and  $H_0 t_0 \simeq 2/3$ ), as well as the size of the voids, affect the cosmic shear and thus the backreaction in the spherically symmetric inhomogeneous Lemaître-Tolman-Bondi or LTB dust models.
2. How the exact backreaction of the void-wall configuration relates to the case where the shear is neglected by treating the voids and the walls as separate FRW solutions.

We perform the calculations on a spatial hypersurface at  $t = t_0$  and do not explicitly consider time-dependence (though  $t_0$  can be considered arbitrary).

The systematic study on the role of shear makes our approach different from the previous studies on the dynamical backreaction in the LTB model which have focused on finding profiles that exhibit acceleration of the average expansion [20, 21] or on general properties of the backreaction [22, 23].

The paper is organized as follows. The necessary background of the LTB solution and the Buchert averaging method are introduced in Sects. 2 and 3, respectively. In Sect. 4, we consider the shear and, in Sect. 5, the backreaction for almost compensated LTB voids residing within almost FRW walls. To show that the results do not depend on the compensating overdensity, we discuss uncompensated voids with a monotonically increasing physical matter density profile in Sect. 5.4. Finally, the conclusions are given in Sect. 6.

## 2. LTB solution

The exact spherically symmetric dust solution of general relativity was discovered by Lemaître in 1933 [24] and is now commonly known as the LTB metric:

$$ds^2 = -dt^2 + \frac{[A'(r, t)]^2}{1 - k(r)} dr^2 + A^2(r, t)(d\theta^2 + \sin^2 \theta d\varphi^2), \quad (2.1)$$

where  $A'(r, t) \equiv \partial_r A(r, t)$ ,  $k(r)$  is related to the curvature of the spatial sections and  $A(r, t)$  is determined by the Friedmann-like evolution equation [25]

$$H(r, t) = H_0(r) \left[ \Omega_0(r) \left( \frac{A_0(r)}{A(r, t)} \right)^3 + (1 - \Omega_0(r)) \left( \frac{A_0(r)}{A(r, t)} \right)^2 \right]^{1/2}, \quad (2.2)$$

where  $H(r, t) \equiv \partial_t A(r, t)/A(r, t) \equiv \dot{A}(r, t)/A(r, t)$ ,  $H_0(r) \equiv H(r, t_0)$  and  $\Omega_0(r)$  are boundary condition functions specified on a spatial hypersurface  $t = t_0$  that determine the radial inhomogeneity profile, while the freedom to choose the function  $A_0(r) \equiv A(r, t_0)$  corresponds to the scaling of the  $r$ -coordinate, used in this work to set

$$A_0(r) = r. \quad (2.3)$$

The curvature function  $k(r)$  in the metric (2.1) is related to these by

$$k(r) \equiv H_0^2(r)(\Omega_0(r) - 1)A_0^2(r), \quad (2.4)$$

and the boundary condition function  $\Omega_0(r)$  is related to the physical matter density  $\rho(r, t)$  on the  $t = t_0$  hypersurface as

$$\Omega_0(r) \equiv \frac{8\pi G}{3H_0^2(r)} \frac{\int_{\mathbb{B}(r)} \rho_0(r) d^3x}{\int_{\mathbb{B}(r)} d^3x}, \quad (2.5)$$

where  $\rho_0(r) \equiv \rho(r, t_0)$ . Inversely,  $\rho_0(r)$  can be written in terms of  $\Omega_0(r)$  and  $H_0(r)$  as

$$\rho_0(r) = \frac{3H_0^2(r)}{8\pi G} \Omega_0(r) \left[ 1 + \frac{A_0(r)}{3A_0'(r)} \left( \frac{\Omega_0'(r)}{\Omega_0(r)} + 2 \frac{H_0'(r)}{H_0(r)} \right) \right]. \quad (2.6)$$

We only consider LTB models where the boundary condition functions obey the constraint

$$H_0(r) = \frac{1}{t_0} \left( 1 - \frac{\sqrt{\Omega_0(r)}}{3} \right), \quad (2.7)$$

which approximates the simultaneous Big Bang condition

$$H_0(r) = \frac{1}{t_0} \left[ \frac{\sqrt{1 - \Omega_0(r)} - \Omega_0(r) \operatorname{arsinh} \sqrt{\frac{1 - \Omega_0(r)}{\Omega_0(r)}}}{(1 - \Omega_0(r))^{3/2}} \right], \quad (2.8)$$

such that the  $|\text{error}| < 1.5\%$  in the considered interval  $0 \leq \Omega_0 \leq 1$  and no error at the extremes  $\Omega_0 = 0$  and  $\Omega_0 = 1$ . We use Eq. (2.7) instead of Eq. (2.8) to make analytic calculations possible. The models with (approximately) simultaneous Big Bang form perhaps the most relevant subcase of LTB solutions, because, in these models, the inhomogeneities are growing modes (see [26]) as e.g. the near isotropy of the CMB suggests is also the case in the real universe.

To study the shear in Sect. 4 and the backreaction in Sect. 5, we need the following quantities of the LTB model: the shear scalar

$$\sigma^2(r, t) \equiv \sigma^{\mu\nu} \sigma_{\mu\nu} = \frac{2}{3} \left( \frac{\dot{A}(r, t)}{A(r, t)} - \frac{\dot{A}'(r, t)}{A'(r, t)} \right)^2, \quad (2.9)$$

the volume expansion scalar

$$\theta(r, t) = 2 \frac{\dot{A}(r, t)}{A(r, t)} + \frac{\dot{A}'(r, t)}{A'(r, t)} = \frac{1}{A'(r, t) A^2(r, t)} \frac{\partial}{\partial r} \left( A^2(r, t) \dot{A}(r, t) \right), \quad (2.10)$$

and their expressions on the  $t = t_0$  hypersurface:

$$\sigma^2(r, t_0) = \frac{2}{3} (r H_0'(r))^2, \quad (2.11)$$

$$\theta(r, t_0) = 3H_0(r) + r H_0'(r) = \frac{1}{r^2} \frac{\partial}{\partial r} (r^3 H_0(r)). \quad (2.12)$$

Using the relation (2.7), the shear (2.11) can also be expressed in terms of  $\Omega_0(r)$  as

$$\sigma^2(r, t_0) = \frac{1}{54} \left( \frac{r}{t_0} \right)^2 \frac{(\Omega_0'(r))^2}{\Omega_0(r)}. \quad (2.13)$$

We also have use for the LTB volume element

$$\sqrt{g} dr d\theta d\varphi = \frac{A'(r, t) A^2(r, t) \sin \theta}{\sqrt{1 - k(r)}} dr d\theta d\varphi, \quad (2.14)$$

where  $g$  denotes the determinant of the spatial part of the metric.

## 2.1 The void-wall model

We use the LTB solution to model a configuration that consists of two different regions: a void where  $\Omega_0 \simeq 0$  and a wall where  $\Omega_0 \simeq 1$ , with a smooth transition in between. For this we choose the  $\Omega_0(r)$  profile as follows:

$$\Omega_0(r) = \left(1 - e^{-(r/r_0)^n}\right)^2, \quad (2.15)$$

where  $r_0$  determines the size of the void and  $n$  the sharpness of the spatial transition between the void and the wall. By virtue of the simultaneous Big Bang condition (2.7), Eq. (2.15) implies

$$H_0(r) = \frac{t_0^{-1}}{3} \left(2 + e^{-(r/r_0)^n}\right), \quad (2.16)$$

which tells us that the void expands faster than the wall by a factor of  $3/2$ .

Using LTB models with the void-wall profile (2.15), we can easily join together many voids to construct a model for a *network* of voids. This is because LTB solutions with the profile (2.15) are, up to negligible terms of order  $e^{-(R/r_0)^n}$ ,  $\Omega = 1$  FRW dust solutions outside the void at  $R > r_0$ , all with  $t_0$  as the age of the universe, implying that the different LTB solutions naturally join together in the wall region.

## 2.2 Small $k(r)$ expansion

For a realistic or sub-horizon size void  $r_0 \ll t_0$ , which we next show implies  $|k(r)| \ll 1 \forall r$ . Note, however, that since the Ricci scalar of the spatial sections is given by

$$\mathcal{R} = \frac{2}{A^2(r, t)A'(r, t)} \frac{\partial}{\partial r} (A(r, t)k(r)), \quad (2.17)$$

or at  $t = t_0$  by

$$\mathcal{R}_0 = \frac{2}{r^2} \frac{\partial}{\partial r} (rk(r)), \quad (2.18)$$

the condition  $|k(r)| \ll 1$  does not imply that the spatial curvature is small in the void.

With the conditions (2.3) and (2.7), the curvature function (2.4) becomes

$$k(r) = - \left(\frac{r}{t_0}\right)^2 \underbrace{\left(1 - \frac{1}{3}\sqrt{\Omega_0(r)}\right)^2}_{\leq 1} (1 - \Omega_0(r)). \quad (2.19)$$

For the considered profiles,  $\Omega_0(r)$  rapidly approaches the value  $\Omega_0 = 1$  outside the void or when  $r > r_0$ , thus implying

$$\max(|k(r)|) \simeq \left(\frac{r_0}{t_0}\right)^2 \ll 1. \quad (2.20)$$

As is evident in Eqs. (2.4) and (2.19),  $k(r)$  depends only on the inhomogeneity profile functions  $\Omega_0(r)$  and/or  $H_0(r)$ , but not on their derivatives. Hence the small  $k(r)$  approximation is equally valid for all the profiles considered here regardless of the sharpness of the transition between the void and the wall.

Since  $|k(r)| \ll 1$ , the part of the LTB volume element (2.14) that contains the curvature function  $k(r)$  can be expanded as follows

$$\frac{1}{\sqrt{1-k(r)}} = 1 + \frac{1}{2}k(r) + \mathcal{O}(k^2(r)) . \quad (2.21)$$

Furthermore, Eqs. (2.1), (2.3) and (2.20) imply that the coordinate  $r$  closely measures the proper distance on the spatial hypersurface defined by  $t = t_0$ .

### 3. Scalar averaging

The spatial volume-average of a scalar  $S(x, t)$  is defined as

$$\langle S(x, t) \rangle_{\mathcal{D}} \equiv \frac{\int_{\mathcal{D}} S(x, t) \sqrt{g} d^3x}{\int_{\mathcal{D}} \sqrt{g} d^3x} , \quad (3.1)$$

where  $g$  is the determinant of the spatial metric and  $\mathcal{D}$  is the averaging domain or a region of the spatial sections.

By applying the averaging (3.1) to the scalar parts of the Einstein equation in an irrotational dust universe, we obtain the Buchert equations [12]:

$$3 \frac{\ddot{a}_{\mathcal{D}}(t)}{a_{\mathcal{D}}(t)} = -4\pi G \langle \rho \rangle_{\mathcal{D}}(t) + \mathcal{Q}_{\mathcal{D}}(t) \quad (3.2)$$

$$3 \left( \frac{\dot{a}_{\mathcal{D}}(t)}{a_{\mathcal{D}}(t)} \right)^2 = 8\pi G \langle \rho \rangle_{\mathcal{D}}(t) - \frac{1}{2} \langle \mathcal{R} \rangle_{\mathcal{D}}(t) - \frac{1}{2} \mathcal{Q}_{\mathcal{D}}(t) \quad (3.3)$$

$$\partial_t \langle \rho \rangle_{\mathcal{D}}(t) = -3 \frac{\dot{a}_{\mathcal{D}}(t)}{a_{\mathcal{D}}(t)} \langle \rho \rangle_{\mathcal{D}}(t) , \quad (3.4)$$

where the regional scale factor is defined as

$$a_{\mathcal{D}}(t) \equiv \left( \frac{\int_{\mathcal{D}} \sqrt{g(x^i, t)} d^3x}{\int_{\mathcal{D}} \sqrt{g(x^i, t_0)} d^3x} \right)^{1/3} \quad (3.5)$$

and the backreaction term

$$\mathcal{Q}_{\mathcal{D}}(t) \equiv \frac{2}{3} (\langle \theta^2 \rangle_{\mathcal{D}} - \langle \theta \rangle_{\mathcal{D}}^2) - \langle \sigma^2 \rangle_{\mathcal{D}} \quad (3.6)$$

quantifies the difference of the time evolution of the averages relative to the homogeneous quantities in an FRW dust universe. In what follows, we take the averaging domain to be an origin-centered ball of coordinate radius  $R$ , i.e.  $\mathcal{D} = \mathbb{B}(R)$ , and do not write it explicitly anymore, so from here on for all scalars  $S$ :

$$\langle S \rangle_{\mathcal{D}} = \langle S \rangle_{\mathbb{B}(R)} = \langle S \rangle . \quad (3.7)$$

### 3.1 Averaging in the LTB model

Given the LTB volume element (2.14), we can expand Eq. (3.1) for small  $k(r)$  using the result (2.21):

$$\langle S \rangle = \langle S \rangle_0 + \frac{1}{2} (\langle Sk \rangle_0 - \langle S \rangle_0 \langle k \rangle_0) + \mathcal{O}(k^2), \quad (3.8)$$

where the subscript 0 now refers to averages where  $k(r) = 0$  in the integration measure, that is  $\sqrt{g_0} \equiv A'(r, t)A^2(r, t) \sin \theta$ . Using this notation, the expression of  $\Omega_0(r)$  in Eq. (2.5) can be recognized simply as

$$\Omega_0(r) = \frac{\langle \rho_0(r) \rangle_0}{\rho_{\text{crit}}(r)}, \quad (3.9)$$

where  $\rho_{\text{crit}}(r) \equiv 3H_0^2(r)/8\pi G$ .

## 4. Shear

When the transition between the void and the wall is made sharper by increasing  $n$ , the shear density on the interface grows but it also becomes more localized. This can be seen in Eq. (2.13) and is illustrated in Fig. 1, where we plot  $\sigma^2(r, t_0)$  for a few profiles (2.15) with different values of  $n$ . It is hence a priori unclear how the integrated or volume-averaged shear behaves when  $n$  is varied.

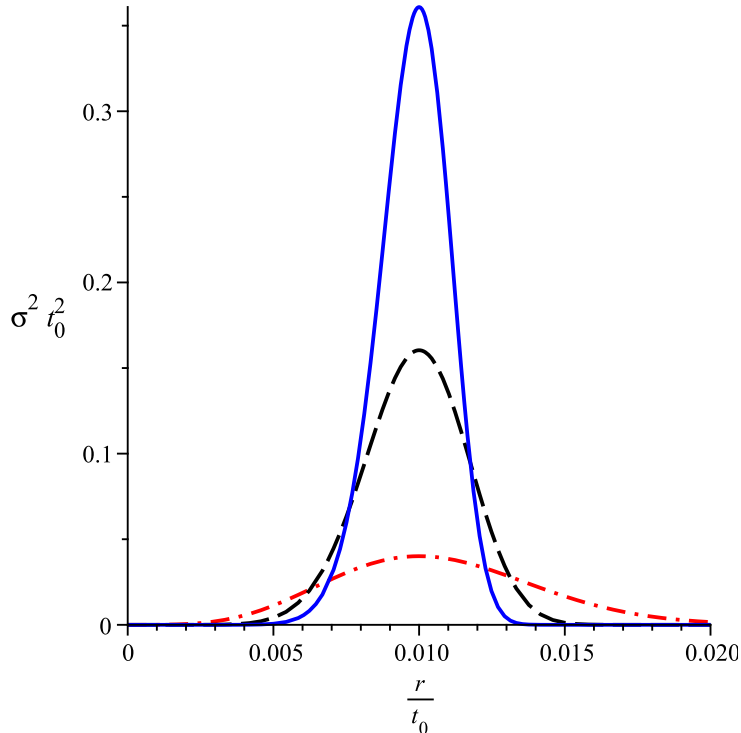


**Figure 1:** Shear distribution as a function of  $r$  for three different values of  $n$ :  $n = 2$  (red dash dot curve),  $n = 4$  (black dashed curve) and  $n = 6$  (blue solid curve). All profiles in this figure have  $r_0 = 0.01t_0$ .

We apply the expansion (3.8) for the shear:

$$\langle \sigma^2 \rangle = \langle \sigma^2 \rangle_0 + \underbrace{\frac{1}{2} (\langle \sigma^2 k \rangle_0 - \langle \sigma^2 \rangle_0 \langle k \rangle_0)}_{\equiv \langle \sigma^2 \rangle_1} . \quad (4.1)$$

Since the shear falls off rapidly in the wall outside the void, we can also make the following approximation

$$\int_0^R \sigma^2(r, t_0) r^2 dr \simeq \int_0^\infty \sigma^2(r, t_0) r^2 dr , \quad (4.2)$$

where  $R > r_0$  is the (coordinate) radius of the spherical averaging region. The validity of the approximation (4.2) depends on  $n$ :  $n = 1$  requires  $R/r_0 \gtrsim 6$ ,  $n = 2$  requires  $R/r_0 \gtrsim 2$ ,  $n = 6$  requires  $R/r_0 \gtrsim 1.2$ , while for very large  $n$  it is enough just to have  $R/r_0 > 1$ ; see Fig. 2.

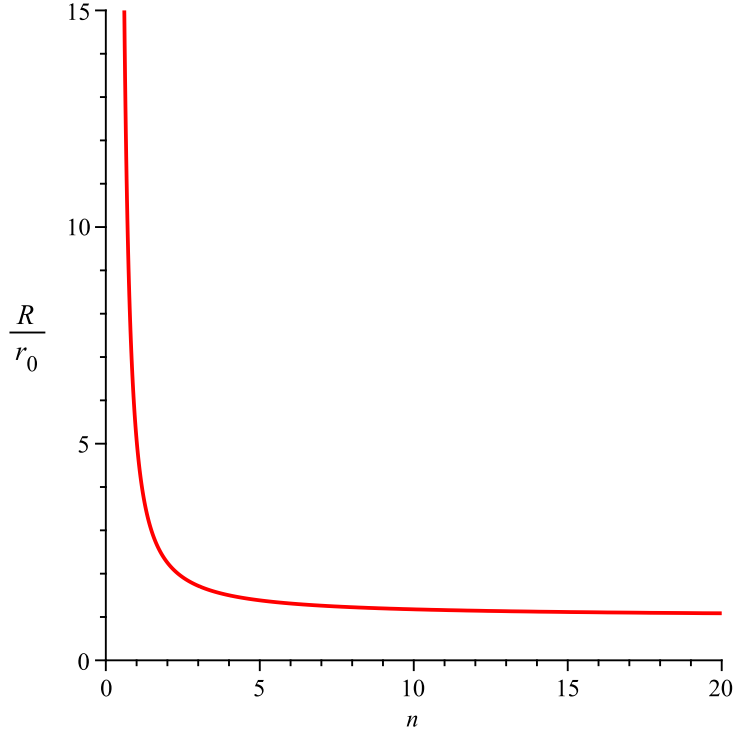


**Figure 2:** The area above the curve (conservatively) represents the region in the parameter space where the approximation (4.2) is valid.

Using Eqs. (2.13), (2.14), (2.15) and (3.1), along with the approximation (4.2), we obtain the following analytic expression for the average shear in the zeroth order of  $k(r)$ :

$$\langle \sigma^2 \rangle_0 = \frac{t_0^{-2}}{6} \left( \frac{r_0}{R} \right)^3 \left( 1 + \frac{3}{n} \right) \Gamma \left( \frac{3}{n} \right) 2^{-3/n} , \quad (4.3)$$



where  $\Gamma$  stands for Euler's gamma function. Similarly, the first order term for shear is

$$\begin{aligned} \langle \sigma^2 \rangle_1 = t_0^{-2} \left( \frac{r_0}{R} \right)^3 \left( \frac{r_0}{t_0} \right)^2 & \left\{ \frac{5}{81} \left( 1 + \frac{5}{n} \right) \Gamma \left( \frac{5}{n} \right) \left[ -8 \cdot 3^{-5/n-2} - 4^{-5/n-1} + 2 \cdot 5^{-5/n-2} + 6^{-5/n-2} \right] \right. \\ & \left. - \left( \frac{r_0}{R} \right)^3 \frac{1}{36n} \left( 1 + \frac{3}{n} \right) \Gamma \left( \frac{3}{n} \right) \Gamma \left( \frac{5}{n} \right) 2^{-3/n} \left[ -8 - 4 \cdot 2^{-5/n} + 2 \cdot 3^{-5/n} + 4^{-5/n} \right] \right\} , \end{aligned} \quad (4.4)$$

which is suppressed by the overall factor  $(r_0/t_0)^2$  relative to the leading order term (4.3). Therefore, as can be easily verified by numerical methods, for the values of  $R/r_0$  and  $n$  above the curve in Fig. 2, Eq. (4.3) gives the correct result for the average shear.

An immediate conclusion from the expression (4.3) is that, for realistic or sub-horizon size voids, the average shear is independent of the size of the void (as long as the volume-ratio  $(r_0/R)^3$  is kept fixed for each void-wall pair). Since, as explained in Sect. 2.1, we can join together many LTB void-wall profiles (2.15) to form a network of voids, Eq. (4.3) thus also gives the average shear for the network of sub-horizon size voids where each void can have a different value of  $r_0$ .

For a universe with half of the volume in voids<sup>1</sup>,  $(r_0/R)^3 = 1/2$ . Using this value and setting  $n = 5$  in Eq. (4.3), we obtain

$$\langle \sigma^2(r, t_0) \rangle = 0.1 t_0^{-2} . \quad (4.5)$$

In the step function limit  $n \rightarrow \infty$ , Eq. (4.3) diverges with the following asymptotics:

$$\langle \sigma^2(r, t_0) \rangle \sim \frac{1}{18} t_0^{-2} \left( \frac{r_0}{R} \right)^3 n , \quad (4.6)$$

telling us that the sharper the transition between the void and the wall, the higher the value of the average shear.

## 5. Backreaction

We consider here the backreaction (3.6) for LTB models with a void-wall profile given by Eqs. (2.15) and (2.16).

### 5.1 Backreaction in 0th order of $k(r)$

Let us first show that the backreaction (3.6) vanishes in the 0th order of  $k(r)$ . For this it is helpful to notice that the following terms can be written as total derivatives:

$$\frac{2}{3} \theta^2 - \sigma^2 = 2 \frac{\dot{A}^2}{A^2} + 4 \frac{\dot{A} \dot{A}'}{A A'} = \frac{2}{A^2 A'} \frac{\partial}{\partial r} \left( \dot{A}^2 A \right) , \quad (5.1)$$

$$\theta = 2 \frac{\dot{A}}{A} + \frac{\dot{A}'}{A'} = \frac{1}{A^2 A'} \frac{\partial}{\partial r} \left( \dot{A} A^2 \right) . \quad (5.2)$$

Since the volume element (2.14) in the 0th order of  $k(r)$  is just

$$\sqrt{g_0} d^3 x = A^2 A' \sin \theta dr d\theta d\varphi , \quad (5.3)$$

---

<sup>1</sup>Order of magnitude consistent with observed values quoted e.g. in Ref. [27].

we have

$$\left\langle \frac{2}{3}\theta^2 - \sigma^2 \right\rangle_0 = \frac{3}{A^3} 2\dot{A}^2 A = 6 \frac{\dot{A}^2(R, t)}{A^2(R, t)} \quad (5.4)$$

and

$$\frac{2}{3}\langle \theta \rangle_0^2 = \frac{2}{3} \left( \frac{3}{A^3} A^2 \dot{A} \right)^2 = 6 \frac{\dot{A}^2(R, t)}{A^2(R, t)}, \quad (5.5)$$

so

$$\mathcal{Q}_0 = \frac{2}{3} (\langle \theta^2 \rangle_0 - \langle \theta \rangle_0^2) - \langle \sigma^2 \rangle_0 = \left\langle \frac{2}{3}\theta^2 - \sigma^2 \right\rangle_0 - \frac{2}{3}\langle \theta \rangle_0^2 = 0. \quad (5.6)$$

Given the zeroth order term of the backreaction (5.6) vanishes, the variance of the expansion rate must be equal to the average shear (4.3) to the leading order, so we have

$$\frac{2}{3} (\langle \theta^2 \rangle_0 - \langle \theta \rangle_0^2) = \frac{t_0^{-2}}{6} \left( \frac{r_0}{R} \right)^3 \left( 1 + \frac{3}{n} \right) \Gamma \left( \frac{3}{n} \right) 2^{-3/n}. \quad (5.7)$$

## 5.2 Backreaction in 1st order of $k(r)$

As the average shear and the variance of the expansion rate cancel exactly in the leading order of  $k(r)$ , we must go beyond the zeroth order to obtain the leading order term of the backreaction.

Using the result (3.8), the backreaction (3.6) becomes

$$\begin{aligned} \mathcal{Q} = \frac{2}{3} (\langle \theta^2 \rangle_0 - \langle \theta \rangle_0^2) - \langle \sigma^2 \rangle_0 + \langle k \rangle_0 & \left( \frac{1}{3} \langle \theta \rangle_0^2 - \frac{1}{2} \left[ \frac{2}{3} (\langle \theta^2 \rangle_0 - \langle \theta \rangle_0^2) - \langle \sigma^2 \rangle_0 \right] \right) + \\ & + \left\langle \left( \frac{\theta^2}{3} - \frac{\sigma^2}{2} \right) k \right\rangle_0 - \frac{2}{3} \langle \theta \rangle_0 \langle \theta k \rangle_0, \end{aligned} \quad (5.8)$$

where, according to the result (5.6),  $\mathcal{Q}_0 \equiv \frac{2}{3} (\langle \theta^2 \rangle_0 - \langle \theta \rangle_0^2) - \langle \sigma^2 \rangle_0$  vanishes, so Eq. (5.8) reduces to

$$\mathcal{Q} = 3H_0^2(R) \langle k \rangle_0 + \left\langle \left( \frac{\theta^2}{3} - \frac{\sigma^2}{2} \right) k \right\rangle_0 - 2H_0(R) \langle \theta k \rangle_0, \quad (5.9)$$

where we have written  $\langle \theta \rangle_0$  in terms of  $H_0(R)$  using the result (5.5).

Using the approximation (4.2) for the integrals in Eq. (5.9) that contain  $k(r)$  as a common factor, we obtain

$$\begin{aligned} \mathcal{Q} = \frac{1}{9} t_0^{-2} \left( \frac{r_0}{R} \right)^3 \left( \frac{r_0}{t_0} \right)^2 \frac{1}{n} \Gamma \left( \frac{5}{n} \right) & \left\{ \frac{8}{9} \cdot 3^{-5/n} - \frac{2}{3} \cdot 4^{-5/n} + \frac{2}{3} \cdot 5^{-5/n} + \frac{4}{9} \cdot 6^{-5/n} + \right. \\ & + e^{-2(R/r_0)^n} \left( -8 - 4 \cdot 2^{-5/n} + 2 \cdot 3^{-5/n} + 4^{-5/n} \right) + \\ & \left. + e^{-(R/r_0)^n} \left( \frac{8}{3} \cdot 2^{-5/n} + \frac{32}{9} \cdot 3^{-5/n} - \frac{7}{3} \cdot 4^{-5/n} - \frac{4}{3} \cdot 5^{-5/n} \right) \right\}. \end{aligned} \quad (5.10)$$

In the limit  $n \rightarrow \infty$ , Eq. (5.10) gives

$$\mathcal{Q} = \frac{4}{135} t_0^{-2} \left( \frac{r_0}{R} \right)^3 \left( \frac{r_0}{t_0} \right)^2, \quad (5.11)$$

showing that although both the average shear and the variance of the expansion rate diverge as  $n \rightarrow \infty$ , the backreaction, given by their difference, has a finite limit. Note that, in the validity region of Fig. 2, the backreaction (5.10) is qualitatively similar for all values of  $n$ , but we consider the step function limit to make comparison with the model that consists of two disjoint FRW solutions in Sect. 5.3.

### 5.3 Comparison with a model that consists of two disjoint FRW solutions

Let us compare the exact solution of the void-wall configuration to a model where the walls and voids are treated as separate FRW regions, following the idea outlined in Ref. [13]. This comparison directly addresses the role of shear since the shear is by construction zero in the disjoint FRW approximation.

For the void or the  $\Omega = 0$  region we use the Milne solution for which

$$\theta_v = \frac{3}{t}, \quad (5.12)$$

and for the wall or the  $\Omega = 1$  region we use the Einstein de Sitter or EdS solution for which

$$\theta_w = \frac{2}{t}. \quad (5.13)$$

Since the shear vanishes in the FRW models, the backreaction is given just by the variance

$$\mathcal{Q}_{\text{FRW}} = \frac{2}{3} (\langle \theta^2 \rangle - \langle \theta \rangle^2), \quad (5.14)$$

where

$$\langle \theta^2 \rangle = \frac{V_w \theta_w^2 + V_v \theta_v^2}{V_w + V_v} \quad (5.15)$$

and

$$\langle \theta \rangle = \frac{V_w \theta_w + V_v \theta_v}{V_w + V_v}. \quad (5.16)$$

By inserting Eqs. (5.12) and (5.13) in Eqs. (5.15) and (5.16), we obtain

$$\mathcal{Q}_{\text{FRW}} = \frac{2}{3} t_0^{-2} f_v (1 - f_v), \quad (5.17)$$

where  $f_v$  is the void fraction:

$$f_v \equiv \frac{V_v}{V_v + V_w}. \quad (5.18)$$

For realistic-sized voids,  $r_0 \ll t_0$ , we have

$$V_v = \frac{4}{3} \pi r_0^3 \left[ 1 + \mathcal{O} \left( \frac{r_0}{t_0} \right)^2 \right] \simeq \frac{4}{3} \pi r_0^3, \quad (5.19)$$

while the wall is spatially flat, so Eq. (5.17) can also be written as

$$\mathcal{Q}_{\text{FRW}} = \frac{2}{3} t_0^{-2} \left( \frac{r_0}{R} \right)^3 \left[ 1 - \left( \frac{r_0}{R} \right)^3 \right], \quad (5.20)$$

For the void fraction value  $f_v = 1/2$  or  $R = 2^{1/3} r_0$ , the backreaction (5.20) gets its maximum value:

$$\mathcal{Q}_{\text{FRW}} = \frac{1}{6} t_0^{-2}. \quad (5.21)$$

We can compare this to the LTB result by setting  $R = 2^{1/3} r_0$  likewise in Eq. (5.11):

$$\mathcal{Q} = \frac{2}{135} t_0^{-2} \left( \frac{r_0}{t_0} \right)^2, \quad (5.22)$$

implying the discrepancy:

$$\mathcal{Q} = \frac{4}{45} \left( \frac{r_0}{t_0} \right)^2 \mathcal{Q}_{\text{FRW}} . \quad (5.23)$$

The result (5.23) demonstrates how important it can be to take into account the shear: for a realistic-sized void with  $r_0 = 0.01t_0$ , the FRW approximation overestimates the backreaction by the tremendous factor of  $10^5$ . The suppressive factor  $(r_0/t_0)^2$  appears to be consistent with the results from perturbative analysis in Refs. [16, 19].

#### 5.4 Uncompensated voids

The void-wall profiles (2.15) considered in Sects. 4–5.3 have a compensating overdense peak in the matter density between the void and the wall regions; see Fig. 3. The peak is required to make the wall (very close to) a flat FRW region, as can be seen from Eqs. (2.6) and (3.9). In this section, we consider profiles without the peak to see whether it plays an important role in suppressing the backreaction relative to the FRW value as in Eq. (5.23).

Instead of specifying  $\Omega_0(r)$  and  $t_0$ , a simultaneous Big Bang LTB model can alternatively be parameterized by the physical matter density profile  $\rho_0(r)$  on a spatial hypersurface at  $t = t_0$ . In this way, we can avoid the compensating overdensity by choosing a monotonically increasing density profile such as

$$\rho_0(r) = \rho_{\text{crit}}(\infty) \left( 1 - e^{-(r/r_0)^n} \right) , \quad (5.24)$$

where  $\rho_{\text{crit}}(\infty) = 1/6\pi G t_0^2$ . Substituting Eqs. (2.7) and (5.24) in Eq. (2.5), we obtain

$$\Omega_0(r) = \frac{9}{4} \left( 1 - \sqrt{1 - \frac{8}{3\sqrt{3}} \sqrt{\sum_{l=1}^{\infty} \frac{(-1)^{l+1} (r/r_0)^{nl}}{l!(nl+3)}}} \right)^2 , \quad (5.25)$$

which, by virtue of Eq. (2.7), implies

$$H_0(r) = \frac{t_0^{-1}}{2} \left( 1 + \sqrt{1 - \frac{8}{3\sqrt{3}} \sqrt{\sum_{l=1}^{\infty} \frac{(-1)^{l+1} (r/r_0)^{nl}}{l!(nl+3)}}} \right) . \quad (5.26)$$

In the step function limit  $n \rightarrow \infty$ , Eqs. (5.25) and (5.26) become

$$\Omega_0(r) = \frac{9}{4} \left( 1 - \sqrt{1 - \frac{8}{9} \sqrt{1 - \left( \frac{r_0}{r} \right)^3}} \right)^2 \Theta(r - r_0) \quad (5.27)$$

and

$$H_0(r) = t_0^{-1} \left[ 1 - \frac{1}{2} \left( 1 - \sqrt{1 - \frac{8}{9} \sqrt{1 - \left( \frac{r_0}{r} \right)^3}} \right) \Theta(r - r_0) \right] , \quad (5.28)$$

where  $\Theta(r - r_0) = \lim_{n \rightarrow \infty} (1 - e^{-(r/r_0)^n})$  stands for the Heaviside step function.

The backreaction (3.6) cannot be integrated analytically for the profile (5.24). Instead, performing the integrals numerically for the parameter values  $(r_0/R)^3 = 1/2$  and  $r_0 = 0.01t_0$ , we obtain

$$\mathcal{Q} = 1.6 \cdot 10^{-6} t_0^{-2} . \quad (5.29)$$

This differs very little from the case with the step function in  $\Omega_0(r)$  and the compensating overdensity in the matter distribution: for comparison, substituting the values  $(r_0/R)^3 = 1/2$  and  $r_0 = 0.01t_0$  in Eq. (5.22) yields

$$\mathcal{Q} = 1.5 \cdot 10^{-6} t_0^{-2} . \quad (5.30)$$

The near equality of the results (5.29) and (5.30) implies that the suppression factor appearing in Eq. (5.23) is not due to the overdense peak between the wall and the void regions. Furthermore, keeping the void-wall volume ratio fixed to  $(r_0/R)^3 = 1/2$  and varying  $r_0$  shows that the dependence of the backreaction on  $r_0$  is very similar to Eq. (5.22), i.e.  $\mathcal{Q} \propto r_0^2$  also for the profile (5.24).

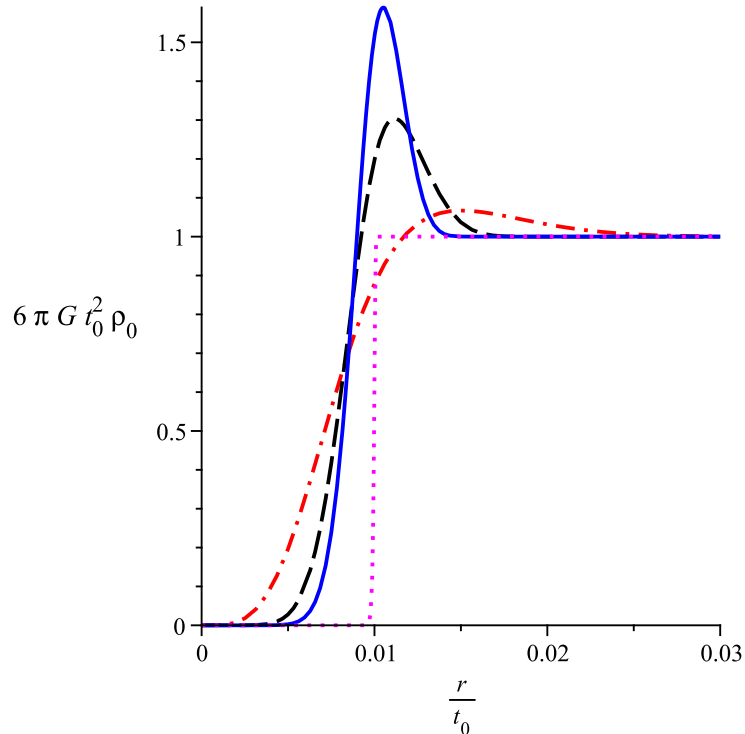


**Figure 3:** Matter density as a function of  $r$  for the profile (5.24) with  $n \rightarrow \infty$  (magenta dotted curve) and the profile (2.15) with three different values of  $n$ :  $n = 2$  (red dash dotted curve),  $n = 4$  (black dashed curve),  $n = 6$  (blue solid curve). All profiles in this figure have  $r_0 = 0.01t_0$ .

Extrapolating the result from a void-wall pair to the network of voids is harder for the uncompensated voids than for the compensated ones. The reason is that, without the compensating overdensity, the solution approaches FRW metric slower: although the

matter density is constant outside the void ( $r > r_0$ ) for the profile (5.24) in the limit  $n \rightarrow \infty$ , the spatial curvature becomes (nearly) constant only much further ( $r \gtrsim 10r_0$ ) from the void. It thus appears that in order to match together uncompensated voids in the simple fashion explained in Sect. 2.1, the separation between the voids must be so large that only a few voids fit inside the horizon. Therefore, more sophisticated junction conditions need to be applied in joining together uncompensated voids to obtain a global void-fraction more consistent with observations such as the ones quoted in Ref. [27].

## 6. Conclusions

We have considered the role of shear in the cosmological backreaction problem using the spherically symmetric LTB dust solution. The LTB models utilized in Sects. 4–5.3 have a close to simultaneous Big Bang with the inhomogeneity profile (2.15) that at  $t = t_0$  interpolates between a void region (where  $\Omega_0 \simeq 0$  and  $H_0 t_0 \simeq 1$ ) and a wall region (where  $\Omega_0 \simeq 1$  and  $H_0 t_0 \simeq 2/3$ ) with the parameters  $r_0$  and  $n$  describing the size of the void and the sharpness of the transition between the two regions, respectively.

For realistic-sized voids ( $r_0 \ll t_0$ ) with a fixed void-wall volume ratio, the results of Sect. 4 show that the volume-average shear is independent of  $r_0$  or the size of the void. This, along with the fact that the different void-wall solutions naturally join together in the EdS-like wall region, implies that the volume-average shear found for a single void-wall pair actually applies also for a *network* of voids of different size. Moreover, we found that for values  $n \gtrsim 10$  both the volume-average shear and the variance of the expansion rate grow proportional to  $n$ , hence diverging in the limit  $n \rightarrow \infty$ . However, as shown in Sect. 5, the backreaction, given by the difference of the variance and the shear, has a finite limiting value for  $n \rightarrow \infty$ .

In Sect. 5.3, to estimate the role of the shear in the backreaction, we compared the LTB result for the backreaction in the limit  $n \rightarrow \infty$  to a simplified model that ignores the shear by approximating the void-wall configuration with two disjoint FRW solutions:  $\Omega_0 = 0$  or the Milne solution for the void and  $\Omega_0 = 1$  or the EdS solution for the wall. The comparison shows that the backreaction obtained using the exact LTB solution is suppressed by at least a factor of  $(r_0/t_0)^2$  relative to the value obtained from the model made up of the separate FRW solutions, hence implying that the shear plays a crucial role here. In Sect. 5.4, we demonstrated that the suppression is not due to a compensating overdensity between the void and the wall regions.

The LTB-based void-wall models considered here contain various simplifications that may misestimate the backreaction of the real universe. Firstly, the models lack globally significant spatial curvature which is known to be important for large backreaction [9]. Large negative spatial curvature can arise in the late universe if its volume becomes dominated by uncompensated voids. This can be seen by realizing that a dense enough network of uncompensated voids is dynamically similar to a huge negatively curved void of size  $r_0/t_0 \simeq \mathcal{O}(1)$ . Another issue is the spherical symmetry of the voids which is obviously broken in the real universe. Finally, the models considered here do not contain collapsing

regions, which have been suggested to play an essential role in the average dynamics of the universe [13, 14].

Besides the dynamical backreaction (3.6) studied in this work, the cosmological structures may have other effects on the observations that are not captured by a spatial averaging procedure. Proposed examples include effects on the propagation of light [10, 28–32] and effects due to our non-average location in the universe [11, 15, 33, 34]. Therefore, small dynamical backreaction does not alone imply that the effects of the inhomogeneities on the observations were small or insignificant.

## Acknowledgments

We thank David Wiltshire and Charles Hellaby for helpful discussions and Tomi Koivisto for useful comments. This work was supported by the Marsden fund of the Royal Society of New Zealand. MM is supported by the Graduate School in Particle and Nuclear Physics (GRASPANP) and acknowledges The Magnus Ehrnrooth foundation for supporting her visit in the University of Canterbury, where the major part of this work was done, and David Wiltshire for hospitality. TM acknowledges The Emil Aaltonen foundation for support.

## References

- [1] G. F. R. Ellis, “Relativistic cosmology: its nature, aims and problems”, p. 215 in *General Relativity and Gravitation*, edited by B. Bertotti, F. de Felice, & A. Pascolini, D. Reidel Publishing Company, 1984.
- [2] G. F. R. Ellis and W. Stoeger “The ‘fitting problem’ in cosmology”, 1987 *Class. Quant. Grav.* **4** 1697
- [3] G. F. R. Ellis, “83 years of general relativity and cosmology: Progress and problems”, *Class. Quant. Grav.* **16** (1999) A37.
- [4] S. Räsänen, “Applicability of the linearly perturbed FRW metric and Newtonian cosmology”, *Phys. Rev. D* **81** (2010) 103512 [arXiv:1002.4779 [astro-ph.CO]].
- [5] A. G. Riess *et al.*, “New Hubble Space Telescope Discoveries of Type Ia Supernovae at  $z > 1$ : Narrowing Constraints on the Early Behavior of Dark Energy”, *Astrophys. J.* **659** (2007) 98 [arXiv:astro-ph/0611572].
- [6] W. J. Percival *et al.*, “Baryon Acoustic Oscillations in the Sloan Digital Sky Survey Data Release 7 Galaxy Sample”, *Mon. Not. Roy. Astron. Soc.* **401** (2010) 2148 [arXiv:0907.1660 [astro-ph.CO]].
- [7] E. Komatsu *et al.*, “Seven-Year Wilkinson Microwave Anisotropy Probe (WMAP) Observations: Cosmological Interpretation”, arXiv:1001.4538 [astro-ph.CO].
- [8] S. Sarkar, “Is the evidence for dark energy secure?”, *Gen. Rel. Grav.* **40** (2008) 269 [arXiv:0710.5307 [astro-ph]].
- [9] T. Buchert, “Dark Energy from Structure - A Status Report”, *Gen. Rel. Grav.* **40** (2008) 467 [arXiv:0707.2153 [gr-qc]].
- [10] T. Mattsson, “Dark energy as a mirage”, *Gen. Rel. Grav.* **42** (2010) 567 [arXiv:0711.4264 [astro-ph]].

- [11] D. L. Wiltshire, “Dark energy without dark energy”, arXiv:0712.3984 [astro-ph].
- [12] T. Buchert, “On average properties of inhomogeneous fluids in general relativity. I: Dust cosmologies”, *Gen. Rel. Grav.* **32** (2000) 105 [arXiv:gr-qc/9906015].
- [13] S. Räsänen, “Accelerated expansion from structure formation”, *JCAP* **0611** (2006) 003 [arXiv:astro-ph/0607626].
- [14] S. Räsänen, “Evaluating backreaction with the peak model of structure formation”, *JCAP* **0804** (2008) 026 [arXiv:0801.2692 [astro-ph]].
- [15] D. L. Wiltshire, “Cosmic clocks, cosmic variance and cosmic averages”, *New J. Phys.* **9** (2007) 377 [arXiv:gr-qc/0702082].
- [16] A. Gruzinov, M. Kleban, M. Porrati and M. Redi, “Gravitational Backreaction of Matter Inhomogeneities”, *JCAP* **0612** (2006) 001 [arXiv:astro-ph/0609553].
- [17] A. Paranjape and T. P. Singh, “Cosmic Inhomogeneities and the Average Cosmological Dynamics”, *Phys. Rev. Lett.* **101** (2008) 181101 [arXiv:0806.3497 [astro-ph]].
- [18] I. A. Brown, G. Robbers and J. Behrend, “Averaging Robertson-Walker Cosmologies”, *JCAP* **0904** (2009) 016 [arXiv:0811.4495 [gr-qc]].
- [19] D. Baumann, A. Nicolis, L. Senatore and M. Zaldarriaga, “Cosmological Non-Linearities as an Effective Fluid”, arXiv:1004.2488 [astro-ph.CO].
- [20] C. H. Chuang, J. A. Gu and W. Y. Hwang, “Inhomogeneity-Induced Cosmic Acceleration in a Dust Universe”, *Class. Quant. Grav.* **25** (2008) 175001 [arXiv:astro-ph/0512651].
- [21] A. Paranjape and T. P. Singh, “The Possibility of Cosmic Acceleration via Spatial Averaging in Lemaitre-Tolman-Bondi Models”, *Class. Quant. Grav.* **23** (2006) 6955 [arXiv:astro-ph/0605195].
- [22] R. A. Sussman, “On the spatial volume averaging in Lemaitre-Tolman-Bondi dust models. 1. Back reaction, spatial curvature and binding energy”, arXiv:0807.1145 [gr-qc].
- [23] R. A. Sussman, “Quasi-local variables, non-linear perturbations and back-reaction in spherically symmetric spacetimes”, arXiv:0809.3314 [gr-qc].
- [24] G. Lemaître, *Annales Soc. Sci. Brux. Ser. I Sci. Math. Astron. Phys. A* **53** (1933) 51.  
For an English translation, see:  
G. Lemaître, “The Expanding Universe”, *Gen. Rel. Grav.* **29** (1997) 641.
- [25] K. Enqvist and T. Mattsson, “The effect of inhomogeneous expansion on the supernova observations”, *JCAP* **0702** (2007) 019 [arXiv:astro-ph/0609120].
- [26] J. Silk, “Large-scale inhomogeneity of the Universe - Spherically symmetric models”, *Astron. Astrophys.* **59** (1977) 53
- [27] F. Hoyle and M. S. Vogeley, “Voids in the 2dF Galaxy Redshift Survey”, *Astrophys. J.* **607** (2004) 751 [arXiv:astro-ph/0312533].
- [28] S. Räsänen, “Light propagation in statistically homogeneous and isotropic dust universes”, *JCAP* **0902** (2009) 011 [arXiv:0812.2872 [astro-ph]].
- [29] K. Enqvist, M. Mattsson and G. Rigopoulos, “Supernovae data and perturbative deviation from homogeneity”, *JCAP* **0909** (2009) 022 [arXiv:0907.4003 [astro-ph.CO]].



- [30] T. Clifton and P. G. Ferreira, “Archipelagian Cosmology: Dynamics and Observables in a Universe with Discretized Matter Content”, *Phys. Rev. D* **80** (2009) 103503 [arXiv:0907.4109 [astro-ph.CO]].
- [31] K. Kainulainen and V. Marra, “A new stochastic approach to cumulative weak lensing”, *Phys. Rev. D* **80** (2009) 123020 [arXiv:0909.0822 [astro-ph.CO]].
- [32] S. Räsänen, “Light propagation in statistically homogeneous and isotropic universes with general matter content”, *JCAP* **1003** (2010) 018 [arXiv:0912.3370 [astro-ph.CO]].
- [33] D. L. Wiltshire, “Cosmological equivalence principle and the weak-field limit”, *Phys. Rev. D* **78** (2008) 084032 [arXiv:0809.1183 [gr-qc]].
- [34] D. L. Wiltshire, “Average observational quantities in the timescape cosmology”, *Phys. Rev. D* **80** (2009) 123512 [arXiv:0909.0749 [astro-ph.CO]].